ARTICLES
PUBLISHED ONLINE: 4 SEPTEMBER 2011 | DOI: 10.1038/NCHEM.1132
nature chemistry

Observation of Fe(v)=O using variable-temperature mass spectrometry and its enzyme-like C–H and C=C oxidation reactions

Irene Prat[1†], Jennifer S. Mathieson[2†], Mireia Güell[1,3], Xavi Ribas[1], Josep M. Luis[1,3], Leroy Cronin[2*] and Miquel Costas[1*]

Oxo-transfer chemistry mediated by iron underpins many biological processes and today is emerging as synthetically very important for the catalytic oxidation of C–H and C=C moieties that are hard to activate conventionally. Despite the vast amount of research in this area, experimental characterization of the reactive species under catalytic conditions is very limited, although a Fe(v)=O moiety was postulated. Here we show, using variable-temperature mass spectrometry, the generation of a Fe(v)=O species within a synthetic non-haem complex at −40 °C and its reaction with an olefin. Also, with isotopic labelling we were able both to follow oxygen-atom transfer from H_2O_2/H_2O through Fe(v)=O to the products and to probe the reactivity as a function of temperature. This study pioneers the implementation of variable-temperature mass spectrometry to investigate reactive intermediates.

For small-molecule activation processes, iron is the element of choice, selected by nature to perform a number of chemically challenging oxidative processes with high precision and reaction rates. Iron-based enzymes, such as cytochrome P450 (ref. 1) and Rieske dioxygenases[2], use O_2 to catalyse highly selective C–H and C=C oxidation reactions, key steps in the metabolic synthesis of metabolites, xenobiotic degradation and other crucial functions. At the heart of these transformations, it is proposed that the catalytic iron centre forms a highly oxidizing oxo-iron species (Fig. 1)[3]. In P450 the active species, formally Fe(v)=O, is best described as an oxo-Fe(iv)-porphyrin radical cation[1], but in the case of the Rieske dioxygenases family of enzymes, which lack the redox non-innocent porphyrin ligand, one postulation is that an oxo-iron(v) species is the reactive species[4,5]. Observation of these highly reactive intermediates remains a formidable challenge that was achieved recently for P450 (refs 6,7), but so far this has not been possible for a non-haem enzyme[8,9].

Functional models of non-haem iron-dependent oxygenases are currently the focus of intense research efforts because of the major challenges in modern synthetic chemistry presented by selective and environmentally benign C–H hydroxylation and olefin *cis*-dihydroxylation reactions[10–13]. In addition, such studies aim to provide an intimate understanding of the processes that underpin the enzymatic reactions. Mechanistic studies of naphthalene 1,2-dioxygenase[9,14], a member of the Rieske dioxygenases family, and of model compounds[15–20] point strongly towards the involvement of a highly electrophilic oxo-iron(v) species, but direct evidence under catalytic conditions is lacking. Recently, the first example of a non-haem oxo-iron(v) species was characterized spectroscopically. This compound contained a tetraanionic ligand, which is likely to quench its electrophilicity, and shows neither C–H hydroxylation nor C=C *cis*-dihydroxylation reactivity[21].

In this respect, variable-temperature mass spectrometry (VT-MS) was envisioned as a very powerful technique with which to study highly reactive intermediate species at very low reagent concentrations, without the need for the large product accumulation required for most spectroscopic techniques. VT-MS could also be used to follow the emergence of the reactive species under much colder conditions than normally used in electrospray mass spectrometric experiments, and thus minimize bimolecular decomposition pathways commonly associated with highly reactive species. Therefore, we envisaged that the observation of reactive species may not only be possible by using low-temperature mass spectrometry[22–26], but also that varying the temperature of the cryospray source during the experiment under catalytic conditions may give further insight and evidence of the identity of the reactive intermediate.

To the best of our knowledge, cryospray mass spectrometry has not been used before to follow reactive intermediates, and herein we present a new technique that uses cryospray technology to allow VT-MS. This technique allowed the temperature-controlled trapping and characterization of a Fe(v)=O species that acted as a functional model of Rieske dioxygenases. Isotopic labelling studies were used to provide accurate chemical descriptions of these species and demonstrated atom transfer, via the Fe complex, from the reagent to the product, that is the *cis*-dihydroxylation of an olefin. The data presented in this work allowed us to elucidate the nature of the iron-based species responsible for performing alkane hydroxylation and olefin *cis*-dihydroxylation in a synthetic biomimetic system.

Results and discussion

The non-haem iron complex **1**, $[Fe(OTf)_2(^{Me,H}Pytacn)]$ (^{Me,H}Pytacn = 1-(2′-pyridylmethyl)-4,7-dimethyl-1,4,7-triazacyclononane, OTf = OSO_2CF_3, Fig. 2), catalyses the hydroxylation of alkanes and the *cis*-dihydroxylation of alkenes using H_2O_2 as oxidant, and thus it constitutes a functional model of the Rieske dioxygenases family of enzymes[18,19]. The hydroxylation of *cis*-1,2-dimethylcyclohexane is stereospecific and affords a racemic

[1]Departament de Química, Universitat de Girona, Campus de Montilivi, Girona 17071, Spain, [2]WestCHEM, School of Chemistry, The University of Glasgow, Glasgow G12 8QQ, UK, [3]Institut de Química Computacional, Universitat de Girona, Campus de Montilivi, Girona 17071, Spain; †These authors contributed equally to this work. *e-mail: miquel.costas@udg.edu; L.Cronin@chem.gla.ac.uk

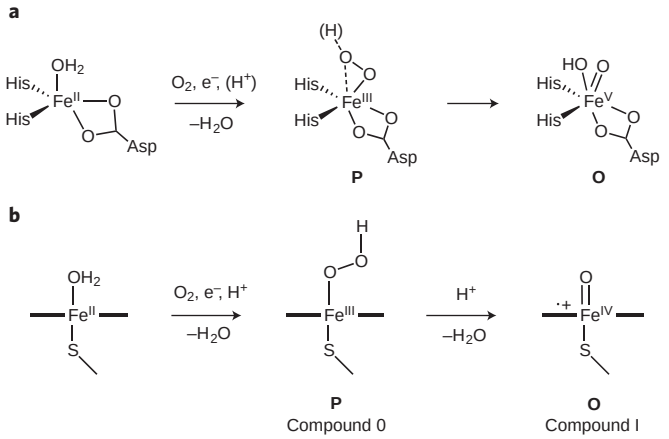

Figure 1 | Mechanistic proposals for the formation of formally oxo-iron(v) species. a, Rieske dioxygenases (non-haem enzyme). **b**, Cytochrome P450 (haem enzyme). **P** refers to the (hydro)peroxide type of species (also known as compound 0 in cytochrome P450) and **O** refers to the formally oxo-iron(v) species (in the case of cytochrome P450, this compound is best described as an oxo-Fe(IV)-porphyrin radical cation, and is known as compound I). His = histidine, Asp = aspartate anion.

mixture of (1*R*,2*R*)-dimethylcyclohexanol and (1*S*,2*S*)-dimethylcyclohexanol (Fig. 2). Similarly, oxidation of *cis*-2-heptene by **1** is *syn*-stereospecific and affords a 2:1 racemic mixture of 95% *erythro*-heptane-2,3-diol and 2-butyl-3-methyloxirane (97% *cis*). When the catalytic reactions were performed in the presence of $H_2{}^{18}O$, the oxidized products exhibited a correspondingly large content of ^{18}O (Fig. 2); alcohols (1*R*,2*R*)-dimethylcyclohexanol and (1*S*,2*S*)-dimethylcyclohexanol were $76 \pm 3\%$ ^{18}O-labelled, but *erythro*-diol was $84 \pm 3\%$ $^{16}O^{18}O$-labelled, which provided evidence that one of the two oxygen atoms in the major part of the diol derived from H_2O. The complementary experiment using $H_2{}^{18}O_2$ as oxidant showed that the second oxygen atom was derived from the peroxide. The isotopic pattern observed in the *cis*-dihydroxylation and C–H hydroxylation reactions did not change within experimental error when reactions were carried out under N_2.

The isotopic labelling experiments, in combination with density functional theory (DFT) computational methods, allowed us to propose confidently that a Fe(v)(O)(OH) species is responsible for the C–H and C=C oxidation events[18,19]. Previously, such a mechanistic scenario was proposed for related non-haem iron catalysts[15–17,20], and a metastable $S = 1/2$ species assigned to Fe(v) was observed recently in catalytic epoxidation low-temperature reactions of non-haem iron complexes with peracids[27]. However, no direct spectroscopic evidence of the putative high-valent species, with the benefit of isotopic labelling, had been obtained so far. The epoxidation reaction mediated by **1** was employed previously to gain indirect product-analysis evidence for the implication of an oxo-iron(v) species[19], but this reaction does not produce kinetically stable epoxide–metal complex intermediates. In addition, the reaction appears to be quite sensitive to the presence of O_2. The inability to isolate completely the cryospray instrument meant an inert atmosphere could not be achieved to probe the reaction mechanism without the presence of O_2. As a result of these limitations, the epoxidation was not studied in the present research.

Monitoring of the reaction of **1** with H_2O_2 by ultraviolet–visible spectroscopy in a range of temperatures from room temperature to $-40\,^{\circ}C$ did not lead to the accumulation or observation of any intermediate species competent for alkane or alkene substrate oxidation. Therefore, the reaction was explored between room temperature and $-40\,^{\circ}C$ using cryospray VT-MS with the aim to observe the elusive reaction intermediates that could be present at low and presumably steady-state concentrations. The VT-MS analysis of the reaction of **1** with H_2O_2 (100 equiv.) between 20 °C and $-40\,^{\circ}C$ showed the growth of a prominent peak at $m/z = 470.1$ that was assigned to $\{[Fe(III)(OH)(^{Me,H}Pytacn)](OTf)\}^+$ (**2**) and a second, less-intense peak at $m/z = 486.1 = M$, which could be formulated as $\{[Fe(III)(OOH)(^{Me,H}Pytacn)](OTf)\}^+$ (**3P**) or $\{[Fe(V)(O)(OH)(^{Me,H}Pytacn)](OTf)\}^+$ (**3O**) on the basis of its m/z and isotopic distribution ratio. This second peak was not observed when reactions were performed at room temperature, and it disappeared rapidly as the temperature was raised from $-40\,^{\circ}C$ to room temperature. This directly implied that **3** was a metastable reaction intermediate (Fig. 3).

To distinguish between the two possible formulations for **3**, isotopic labelling experiments were conducted. As a result of the consistency of our experiments with catalytic reactions, and also the experimental limitations of the isotopically labelled reagents ($H_2{}^{18}O_2$ is a 2% weight/weight solution in water), we studied (i) the reaction of **1** with $H_2{}^{16}O_2$ (10 equiv.) in the presence of $H_2{}^{18}O$ (1,000 equiv.), (ii) the complementary experiment that involved the reaction of **1** with $H_2{}^{18}O_2$ (10 equiv.) in the presence of H_2O (1,000 equiv.) and (iii) the reaction of **1** with $H_2{}^{18}O_2$ (10 equiv.) in the presence of $H_2{}^{18}O$ (1,000 equiv.). However, because our $H_2{}^{18}O_2$ solutions were 2% in $H_2{}^{16}O$, over 300 equiv. of $H_2{}^{16}O$ were also present in solution in this experiment.

Most remarkably, the spectrum of the reaction of **1** with $H_2{}^{16}O_2$ in the presence of $H_2{}^{18}O$ showed a new cluster peak assigned to **3** displaced by two m/z units and centred at $m/z = 488.1 = M + 2$ (Fig. 4b(ii)). The complementary experiment using $H_2{}^{18}O_2$ and $H_2{}^{16}O$ confirmed our initial formulation[18,19], and showed a peak centred at $m/z = 488.1 = M + 2$ (Fig. 4b(iii)). Finally, **3O** was generated by using $H_2{}^{18}O_2$ (10 equiv.) in the presence of $H_2{}^{18}O$ (1,000 equiv.) (Fig. 4b(iv)). In this case, the peak at $m/z = 488.1 = M + 2$ continued to be the major species, but a peak at $m/z = 490.1 = M + 4$ appeared as the second most intense component of the spectrum. The decreased intensity and stability of the ion peaks associated with **3O** in this spectrum (Fig. 4b(iv)) presumably resulted from contamination by other species with m/z values that ranged from 486 to 492, with a higher percentage of species with m/z of 488 present compared to those at 490 m/z, along with contamination

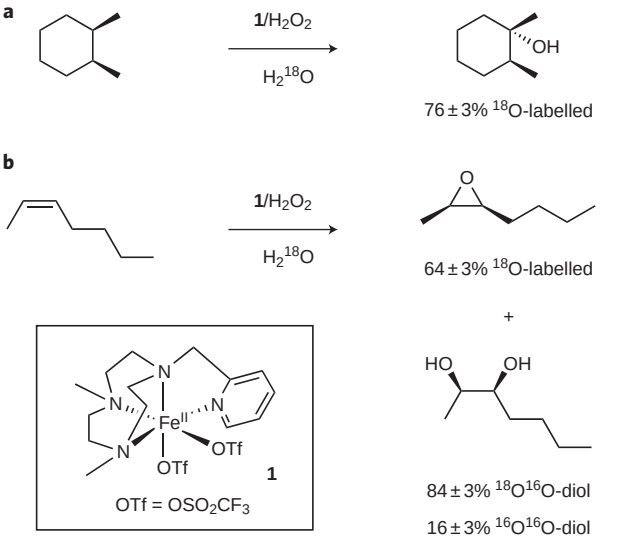

Figure 2 | Complex 1 catalyses the hydroxylation of alkanes and the *cis*-dihydroxylation of alkenes. a,**b**, Stereospecific hydroxylation of *cis*-1,2-dimethylcyclohexane (1,000 equiv.) (**a**) and epoxidation and *cis*-dihydroxylation of 2-heptene (1,000 equiv.) (**b**) with H_2O_2 (10 equiv.) catalysed by **1** in the presence of $H_2{}^{18}O$ (1,000 equiv.).

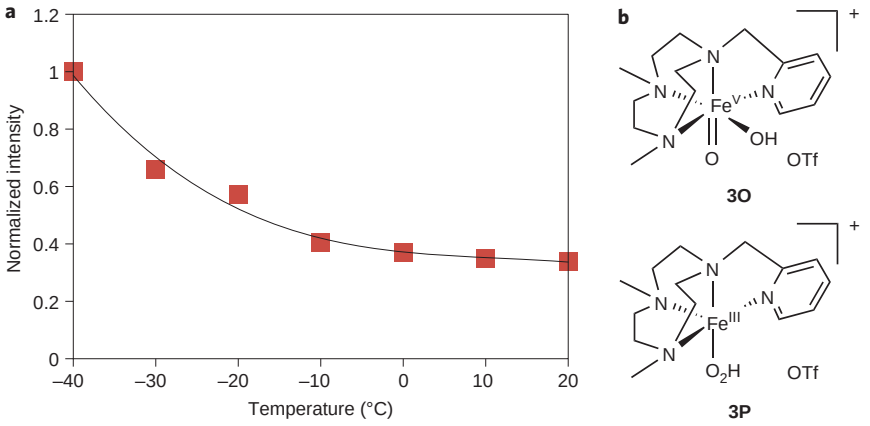

Figure 3 | Change of intensity of 3O or 3P when the temperature is increased from −40 °C to 20 °C. a, The decrease in the normalized intensity of the peak at 486.1 *m/z* as the temperature increases provides evidence that **3O** or **3P** is the metastable intermediate, as these species are not observable at higher temperatures. **b**, Structure of {[Fe(v)(O)(OH)(^{Me,H}Pytacn)](OTf)}$^+$ (**3O**) and {[Fe(iii)(OOH)(^{Me,H}Pytacn)](OTf)}$^+$ (**3P**).

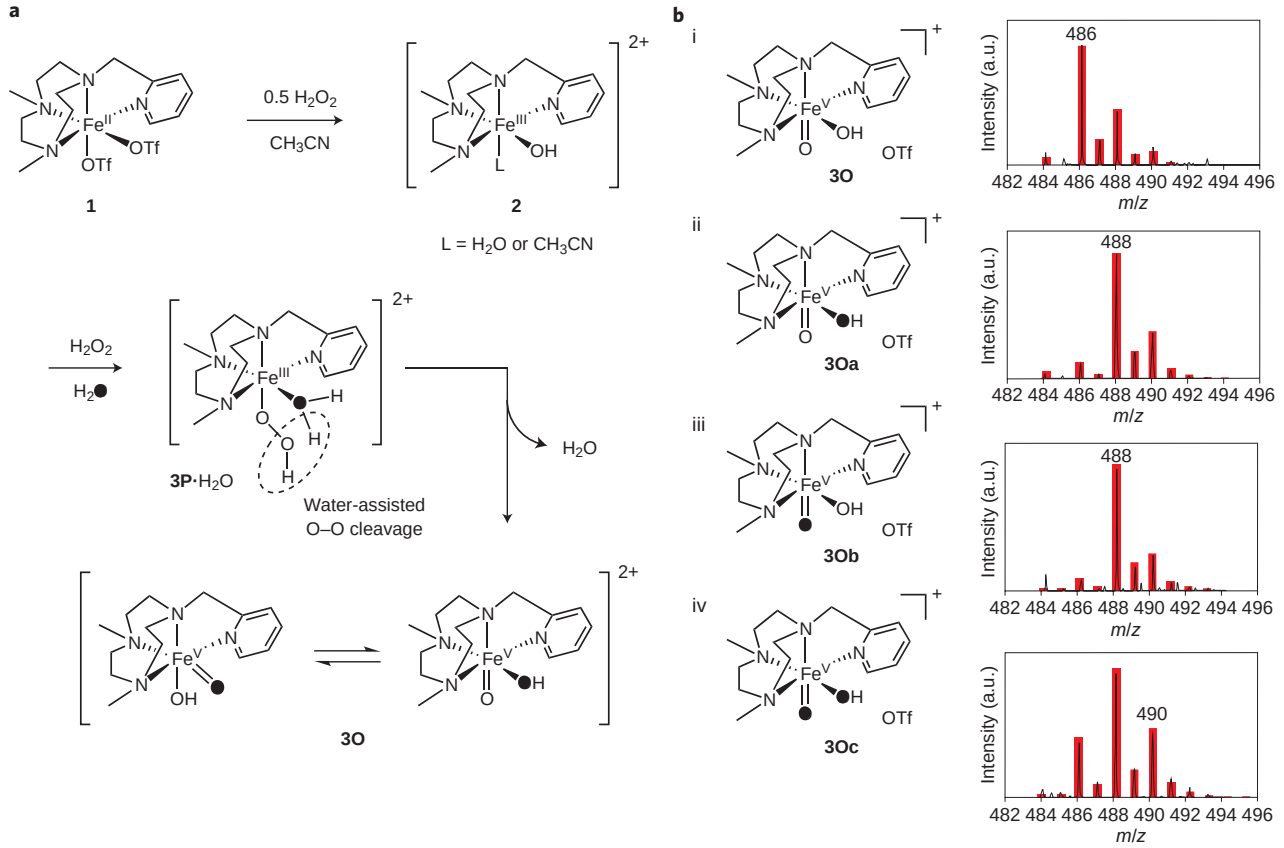

Figure 4 | Mechanisms and shift of mass spectral peaks when $H_2{}^{18}O$ and $H_2{}^{18}O_2$ are used to give the Fe(v)(O)(OH) species. a, The formation of the oxo-iron(v) species {[Fe(v)(O)(OH)(^{Me,H}Pytacn)](OTf)}$^+$ (**3O**) via a water-assisted heterolytic cleavage of the O–O bond in {[Fe(iii)(OOH)(OH_2)(^{Me,H}Pytacn)](OTf)}$^+$ (**3P·H_2O**). **b**, Cryospray ionization mass spectra (CSI-MS) of the species formed when [Fe(ii)(^{Me,H}Pytacn)($OTf)_2$] (**1**) was reacted with H_2O_2 and H_2O in acetonitrile solution at −40 °C. **i**, {[Fe(v)(O)(OH)(^{Me,H}Pytacn)](OTf)}$^+$ (**3O**) generated with $H_2{}^{16}O_2$ (10 equiv.) in the presence of $H_2{}^{16}O$ (1,000 equiv.). **ii**, {[Fe(v)(O)(^{18}OH)(^{Me,H}Pytacn)](OTf)}$^+$ (**3Oa**) (the additional descriptor **a** refers to the isotopic composition of H_2O and H_2O_2 reagents used in the generation of **3O**) generated with $H_2{}^{16}O_2$ (10 equiv.) in the presence of $H_2{}^{18}O$ (1,000 equiv.). **iii**, {[Fe(v)(^{18}O)(OH)(^{Me,H}Pytacn)](OTf)}$^+$ (**3Ob**) generated with $H_2{}^{18}O_2$ (10 equiv.) in the presence of $H_2{}^{16}O$ (1,000 equiv.). **iv**, {[Fe(v)(^{18}O)(^{18}OH)(^{Me,H}Pytacn)](OTf)}$^+$ (**3Oc**) generated with $H_2{}^{18}O_2$ (10 equiv.) in the presence of $H_2{}^{18}O$ (1,000 equiv.). All calculated peaks fit the statistical treatment of experimental error. Red bars correspond to the simulated data (see Supplementary Information for the full analysis of the isotopic envelope) and black lines correspond to the experimental data. ● = 18-labelled oxygen, a.u. = arbitrary units.

from the large amount of water present in the solution. Also, an experiment using D_2O was carried out to show the rationale for the assignment of **3** with the intensity of the 490 *m/z* peak increasing, consistent with the incorporation of D_2O (for a full explanation of the species present in the isotope envelope, see Supplementary Fig. S5).

As peroxide-type species do not exchange their oxygen atoms with water[28], the isotopic labelling observations appeared

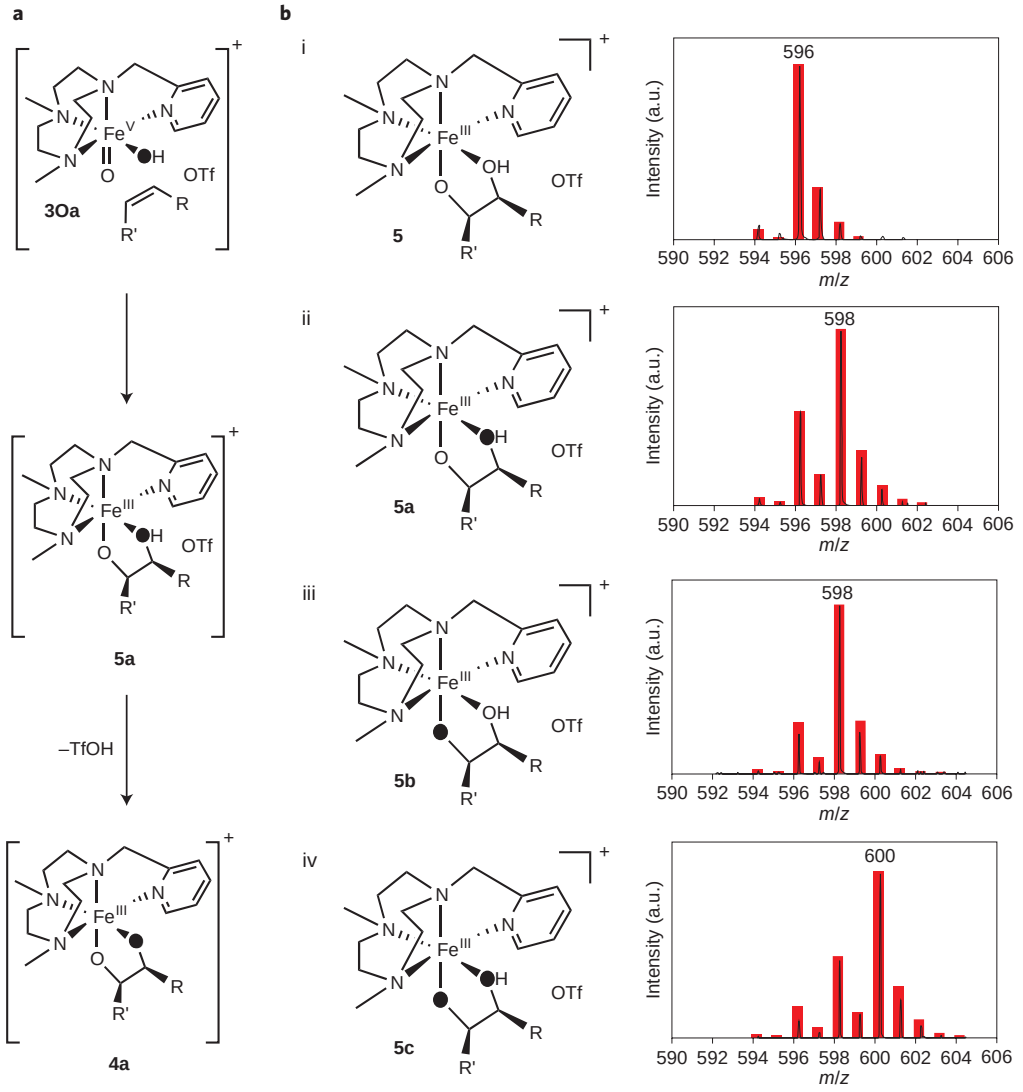

Figure 5 | Mechanisms and shift of mass spectral peaks when $H_2{}^{18}O$ and $H_2{}^{18}O_2$ are used to give the hydrogenglycolates 5 and the glycolates 4. **a**, The reaction between the oxo-iron(v) species {[Fe(v)(O)(OH)(^{Me,H}Pytacn)](OTf)}$^+$ (**3O**) with an olefin to form the hydrogenglycolate species {[Fe(iii)(C_8H_{14}(O)(OH))(^{Me,H}Pytacn)](OTf)}$^+$ (**5**) and glycolate species [Fe(iii)(C_8H_{14}O(O))(^{Me,H}Pytacn)]$^+$ (**4**). **b**, CSI-MS spectra of the species formed when {[Fe(v)(O)(OH)(^{Me,H}Pytacn)](OTf)}$^+$ (**3O**) was reacted with an olefin in acetonitrile solution at −40 °C. **i**, {[Fe(iii)(C_8H_{14}(O)(OH))(^{Me,H}Pytacn)](OTf)}$^+$ (**5**) formed by reaction of cyclooctene (100 equiv.) with {[Fe(v)(O)(OH)(^{Me,H}Pytacn)](OTf)}$^+$ (**3O**) (generated with $H_2{}^{16}O_2$ (3 equiv.) in the presence of $H_2{}^{16}O$ (1,000 equiv.)). **ii**, {[Fe(iii)(C_8H_{14}(O)(^{18}OH))(^{Me,H}Pytacn)](OTf)}$^+$ (**5a**) (the additional descriptor **a** refers to the isotopic composition of H_2O and H_2O_2 reagents used in the generation of **3O**, which in turn form **5**) formed by reaction of cyclooctene (100 equiv.) with {[Fe(v)(O)(^{18}OH)(^{Me,H}Pytacn)](OTf)}$^+$ (**3Oa**) (generated with $H_2{}^{16}O_2$ (3 equiv.) in the presence of $H_2{}^{18}O$ (1,000 equiv.)). **iii**, {[Fe(iii)(C_8H_{14}(^{18}O)(OH))(^{Me,H}Pytacn)](OTf)}$^+$ (**5b**) formed by reacting cyclooctene (100 equiv.) with {[Fe(v)(^{18}O)(OH)(^{Me,H}Pytacn)](OTf)}$^+$ (**3Ob**) (generated with $H_2{}^{18}O_2$ (3 equiv.) in the presence of $H_2{}^{16}O$ (1,000 equiv.)). **iv**, {[Fe(iii)(C_8H_{14}(^{18}O)(^{18}OH))(^{Me,H}Pytacn)](OTf)}$^+$ (**5c**) formed by reacting cyclooctene (100 equiv.) with {[Fe(v)(^{18}O)(^{18}OH)(^{Me,H}Pytacn)](OTf)}$^+$ (**3Oc**) (generated with $H_2{}^{18}O_2$ (3 equiv.) in the presence of $H_2{}^{18}O$ (1,000 equiv.)).

incompatible with **3P**. Instead, the mass spectrometry isotopic labelling experiments provided a strong indication that **3** must be described as {[Fe(v)(O)(OH)(^{Me,H}Pytacn)](OTf)}$^+$ (**3O**), in which a single oxygen atom derived from H_2O_2 and a second oxygen atom derived from H_2O, presumably via a water-assisted heterolytic O–O breakage in the hydroperoxide species {[Fe(iii)(OOH)(OH_2)(^{Me,H}Pytacn)](OTf)}$^+$ (**3P·H_2O**) (Fig. 4a)[29,30]. Isotopic labelling experiments showed that the optimum simulation of the spectra shown in Fig. 4b(ii),(iii) required a contribution of ∼10% from species with $m/z = M + 4$. These species were assigned to {[Fe(iii)(OH)($^{18}OH_2$)(^{Me,H}Pytacn)](OTf)}$^+$ and {[Fe(iii)(^{18}OH)(OH_2)(^{Me,H}Pytacn)](OTf)}$^+$, which correspond to the aqualigated form of **2**. Although the mass spectrometry data do not provide a direct indication of the oxidation state of the iron site, we concluded that Fe(v) was the most plausible oxidation state because of the redox innocence of all the ligands, which is also consistent with DFT analysis of this species[18,19].

With good evidence for the identity of **3O**, we sought to demonstrate its reactivity with respect to an intermolecular oxidation reaction, as this would provide further proof that **3O** is a reactive species, as suggested by our mass spectrometric assignment. To do this, we chose a reaction with an olefin because we envisioned that if **3O** performs an olefin *cis*-dihydroxylation reaction it will form a kinetically stable iron–(hydrogen)glycolate species (Fig. 5a). If so, the use of ^{18}O labels could also be a powerful tool to demonstrate that, indeed, the transformation was mediated by the reactive Fe(v)=O species assigned to the identity of **3O**.

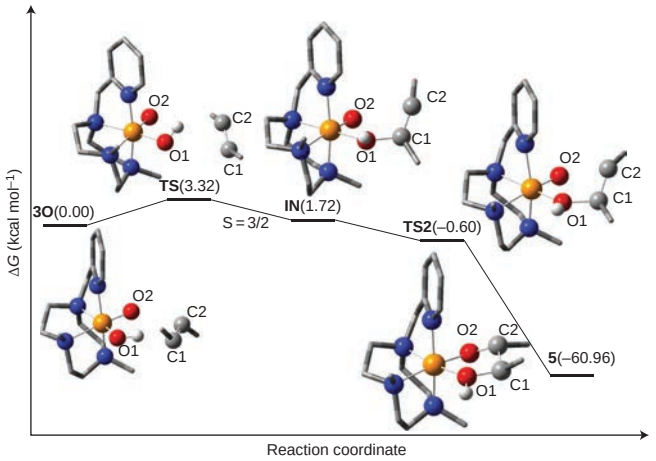

Figure 6 | DFT Gibbs energy profile of the reaction between the oxo-iron(v) species 3O with *trans*-2-butene to form the hydrogenglycolate species 5. Hydrogen atoms on the olefin substrate are omitted for clarity (see Supplementary Methods S16 for full details on the computational methods). TS = transition state.

To this end, **3O** was generated and reacted with cyclooctene (100 equiv.). Mass spectrometry analysis of the reaction indicated that the cluster peak assigned to **3O** disappeared and new peaks at $m/z =$ 446.2 (not shown) and $m/z = 596.2$ (Fig. 5b(i)) emerged. The isotopic pattern of these ions could be simulated successfully as the complexed glycolate species $[Fe(III)(C_8H_{14}O_2)(^{Me,H}Pytacn)]^+$ (**4**) and the complexed hydrogenglycolate species $\{[Fe(III)(C_8H_{14}(O)(OH))(^{Me,H}Pytacn)](OTf)\}^+$ (**5**) (**4** + H^+ + OTf), which resulted from a *cis*-dihydroxylation reaction of **3O** with cyclooctene. (See Supplementary Figs S7 and S8 for the spectrum of dihydroxylation of cyclohexene and 1-octene, respectively.)

Further evidence that **3O** was the reactive intermediate came from isotopic labelling experiments. **3Oa** (the additional descriptor **a** refers to the isotopic composition of H_2O and H_2O_2 reagents used in the generation of **3O**) was generated with $H_2{}^{16}O_2$ in the presence of $H_2{}^{18}O$ (1,000 equiv.) and reacted with cyclooctene (100 equiv.). In this case (Fig. 5b(ii)), the cluster ion associated with $\{[Fe(III)(C_8H_{14}(O)(^{18}OH))(^{Me,H}Pytacn)](OTf)\}^+$ (**5a**) was displaced by two mass units. Similarly, when **3Ob** was generated with $H_2{}^{18}O_2$ in the presence of $H_2{}^{16}O$ (1,000 equiv.) and then reacted with cyclooctene (100 equiv.), the spectrum (Fig. 5b(iii)) showed again the formation of cluster ions at $m/z = 448.2$ (not shown) and $m/z = 598.2$ assigned to $[Fe(III)(C_8H_{14}(^{18}O)(O))(^{Me,H}Pytacn)]^+$ (**4b**) and $\{[Fe(III)(C_8H_{14}(^{18}O)(OH))(^{Me,H}Pytacn)](OTf)\}^+$ (**5b**), respectively. Analogous results were obtained when 1-octene and cyclohexene were chosen as the substrates (see Supplementary Figs S5 and S6). These observations led us to conclude that **3O** constitutes a reaction intermediate that precedes the formation of **4** and **5** on reaction with an olefin.

Gas chromatography (GC) and GC-MS analysis at the end of the low-temperature reaction with cyclooctene showed that the expected epoxides (0.9 turnovers) and diols (1.0 turnovers) were formed. Isotopic patterns and m/z assigned to **4** and **5** could also support alternative epoxide-bound formulations $[Fe(III)(O)(C_8H_{14}O)(^{Me,H}Pytacn)]^+$ for **4** and $\{[Fe(III)(OH)(C_8H_{14}(O))(^{Me,H}Pytacn)](OTf)\}^+$ for **5**. However, it is well known that epoxides are very poor ligands with putative epoxide-bound species that dissociate very fast, and thus are unstable kinetically. Ion peaks that correspond to **4** and **5** remained stable over time and did not show oxygen exchange with water molecules from the reaction mixture. In addition, hydroxide and oxide ligands in thermally stable Fe(III) complexes should engage in water-exchange reactions. Hence, the stability of the ion peaks associated with **4** and **5** against water exchange further discards epoxide-bound formulations. Therefore, we can conclude that epoxide-bound species were not detected in the spectra.

We have described previously, on the basis of DFT computations, that water-assisted transformation of **3P** into **3O** is thermoneutral and has a small (Gibbs energy of activation ($\Delta G^{\ddagger}$) = 20 kcal mol^{-1}) activation barrier[18,19], in good agreement with literature values for related non-haem iron complexes[29,30]. For comparison, homolytic breakage of the O–O bond in the Fenton intermediate $[(H_2O)_5Fe(III)(OOH)]^{2+}$ is computed to have a comparable barrier of 21 kcal mol^{-1} (ref. 31). To substantiate the proposal that the Fe(v)(O)(OH) species is, indeed, the executor of the *cis*-dihydroxylation event, the reaction of **3O** with *trans*-2-butene as a model substrate was also computed using DFT methods. A summary of the DFT results is given in Fig. 6. The dihydroxylation is strongly exergonic, with **5** being 60.96 kcal mol^{-1} more stable than **3O** + *trans*-2-butene. In addition, the reaction proceeds with a very small energy barrier. The ground state of **3O** is $S = 3/2$, and it is well separated in energy (11.50 kcal mol^{-1}) with respect to the first excited state ($S = 1/2$). The attack of the hydroxo-ligand over the olefin leads to the formation of the first C1–O1 bond, to form the intermediate **IN**, with a small barrier of $\Delta G^{\ddagger} = 3.32$ kcal mol^{-1}. **IN** then evolves via attack of the oxo-ligand over C2, with no energy barrier, which leads to the direct formation of the glycolate species **5**. The concerted, yet unsymmetrical, nature of the *cis*-dihydroxylation event derived from our calculations bears a strong resemblance to the analysis described recently by Che and co-workers for the *cis*-dihydroxylation reaction mediated by a non-haem iron complex on reaction with Oxone[32]. However, on the basis of product analyses and DFT calculations, recent proposals suggest that $Fe(IV)(OH)_2$ species could be responsible for the *cis*-dihydroxylation reactions in selected iron catalysts[33–35]. These catalysts exhibit different reactivity patterns with respect to the $[Fe(^{Me,H}Pytacn)]$ system described herein. In the former cases, isotopic analysis shows that *cis*-dihydroxylation preferentially takes place via insertion of two oxygen atoms from a single H_2O_2 molecule.

Further evidence for a different mechanistic scenario was provided by the observation that $[Fe(IV)(O)(OH_2)(^{Me,H}Pytacn)]^{2+}$ does not mediate the *cis*-dihydroxylation of olefins. This complex was prepared recently and spectroscopically characterized by us[36], and computational analyses indicated that a $[Fe(IV)(OH)_2(^{Me,H}Pytacn)]^{2+}$ intermediate is involved in its water-exchange reactions.

In conclusion, the mechanisms that underlie *cis*-dihydroxylation reactions mediated by $[Fe(OTf)_2(^{Me,H}Pytacn)]$ are fundamentally distinct from those that operate through a Fe(II)/Fe(IV) cycle.

Conclusions

Previous computational and product-analysis experiments in catalytic C–H hydroxylation and C=C *cis*-dihydroxylation reactions mediated by non-haem iron catalysts predicted Fe(v)(O)(OH) species as the final oxidant that executes very fast stereospecific C–H and C=C oxidation reactions[15–19,29,30]. With this work we present the development and application of VT-MS to the investigation of the reaction between the non-haem iron catalyst **1** with H_2O_2 at temperatures between 20 and −40 °C, which led to the identification of a metastable intermediate that could be formulated as $\{[Fe(v)(O)(OH)(^{Me,H}Pytacn)](OTf)\}^+$ (**3O**) on the basis of isotopic labelling experiments. Such experiments provide evidence that **3O** contains an oxygen atom from H_2O_2 and a second oxygen atom from water, which in turn constitutes strong evidence for a water-assisted path towards its generation, but direct kinetic proof is not yet available and will be the subject of further studies. Despite this limitation, isotopic labelling experiments demonstrated that **3O** precedes the *cis*-dihydroxylation reaction of olefins.

This study does not provide a full account of the reaction mechanisms that operate when **1** reacts with H_2O_2 and organic substrates, but it does provide experimental evidence, corroborated by a full DFT analysis and isotopic labelling characterization, for the generation of a Fe(V)(O)(OH) species, a powerful oxidant, under conditions relevant to catalysis. Thus, this work provides a new fundamental framework for understanding the nature of the iron-based species responsible for performing alkane hydroxylation and olefin *cis*-dihydroxylation in a synthetic biomimetic system that may have enzymatic relevance. Also, we have demonstrated the potential of VT-MS in the investigation of reactive intermediates.

Received 16 February 2011; accepted 27 July 2011; published online 4 September 2011

References

1. Ortiz de Montellano, P. R. *Cytochrome P450: Structure, Mechanism and Biochemistry* 3rd edn (Kluwer Academic/Plenum, 2005).
2. Ferraro, D. J., Gakhar, L. & Ramaswamy, S. Rieske business: structure–function of Rieske non-heme oxygenases. *Biochem. Biophys. Res. Commun.* **338,** 175–190 (2005).
3. Groves, J. T. High-valent iron in chemical and biological oxidations. *J. Inorg. Biochem.* **100,** 434–447 (2006).
4. Chakrabarty, S., Austin, R. N., Deng, D., Groves, J. T. & Lipscomb, J. D. Radical intermediates in monooxygenase reactions of Rieske dioxygenases. *J. Am. Chem. Soc.* **129,** 3514–3515 (2007).
5. Wolfe, M. D. *et al.* Benzoate 1,2-dioxygenase from *Pseudomonas putida*: single turnover kinetics and regulation of a two-component Rieske dioxygenase. *Biochemistry* **41,** 9611–9626 (2002).
6. Schlichting, I. *et al.* The catalytic pathway of cytochrome P450cam at atomic resolution. *Science* **287,** 1615–1622 (2000).
7. Rittle, J. & Green, M. T. Cytochrome P450 compound I: capture, characterization, and C–H bond activation kinetics. *Science* **330,** 933–937 (2010).
8. Karlsson, A. *et al.* Crystal structure of naphthalene dioxygenase: side-on binding of dioxygen to iron. *Science* **299,** 1039–1042 (2003).
9. Wolfe, M. D., Parales, J. V., Gibson, D. T. & Lipscomb, J. D. Single turnover chemistry and regulation of O_2 activation by the oxygenase component of naphthalene 1,2-dioxygenase. *J. Biol. Chem.* **276,** 1945–1953 (2001).
10. Chen, M. S. & White, M. C. A predictable selective aliphatic C–H oxidation reaction for complex molecule synthesis. *Science* **318,** 783–787 (2007).
11. Chen, M. S. & White, M. C. Combined effects on selectivity in Fe-catalyzed methylene oxidation. *Science* **327,** 566–571 (2010).
12. Gomez, L. *et al.* Stereospecific CH oxidation with H_2O_2 catalyzed by a chemically robust site-isolated iron catalyst. *Angew. Chem. Int. Ed.* **48,** 5720–5723 (2009).
13. Que, L. & Tolman, W. B. Biologically inspired oxidation catalysis. *Nature* **455,** 333–340 (2008).
14. Wolfe, M. D. & Lipscomb, J. D. Hydrogen peroxide-coupled *cis*-diol formation catalyzed by naphthalene 1,2-dioxygenase. *J. Biol. Chem.* **278,** 829–835 (2003).
15. Chen, K. & Que, L. Jr Stereospecific alkane hydroxylation by nonheme iron catalysts: mechanistic evidence for an Fe(V)=O active species. *J. Am. Chem. Soc.* **123,** 6327–6337 (2001).
16. Chen, K., Costas, M., Kim, J., Tipton, A. K. & Que, L. Jr Olefin *cis*-dihydroxylation versus epoxidation by nonheme iron catalysts: two faces of an Fe(III)–OOH coin. *J. Am. Chem. Soc.* **124,** 3026–3035 (2002).
17. Bassan, A., Blomberg, M. R. A., Siegbahn, P. E. M. & Que, L. Jr Two faces of a biomimetic non-heme HO–Fe(V)=O oxidant: olefin epoxidation versus *cis*-dihydroxylation. *Angew. Chem. Int. Ed.* **44,** 2939–2941 (2005).
18. Company, A. *et al.* Alkane hydroxylation by a nonheme iron catalyst that challenges the heme paradigm for oxygenase action. *J. Am. Chem. Soc.* **129,** 15766–15767 (2007).
19. Company, A. *et al.* Olefin-dependent discrimination between two nonheme HO–Fe(V)=O tautomeric species in catalytic H_2O_2 epoxidations. *Chem. Eur. J.* **15,** 3359–3362 (2009).
20. Makhlynets, O. V. & Rybak-Akimova, E. V. Aromatic hydroxylation at a non-heme iron center: observed intermediates and insights into the nature of the active species. *Chem. Eur. J.* **16,** 13995–14006 (2010).
21. de Oliveira, F. T. *et al.* Chemical and spectroscopic evidence for an Fe(V)-oxo complex. *Science* **315,** 835–838 (2007).
22. Markert, C. & Pfaltz, A. Screening of chiral catalysts and catalyst mixtures by mass spectrometric monitoring of catalytic intermediates. *Angew. Chem. Int. Ed.* **43,** 2498–2500 (2004).
23. Feichtinger, D. & Plattner, D. A. Direct proof for O=Mn(V) (salen) complexes. *Angew. Chem. Int. Ed. Engl.* **36,** 1718–1719 (1997).
24. Miras, H. N., Wilson, E. F. & Cronin, L. Unravelling the complexities of inorganic and supramolecular self-assembly in solution with electrospray and cryospray mass spectrometry. *Chem. Commun.* 1297–1311 (2009).
25. Wilson, E. F. *et al.* Probing the self-assembly of inorganic cluster architectures in solution with cryospray mass spectrometry: growth of polyoxomolybdate clusters and polymers mediated by silver(I) ions. *J. Am. Chem. Soc.* **130,** 13876–13884 (2008).
26. Yan, J., Long, D.-L., Wilson, E. F. & Cronin, L. Discovery of heteroatom-embedded Te{W18O54} nanofunctional polyoxometalates by use of cryospray mass spectrometry. *Angew. Chem. Int. Ed.* **48,** 4376–4380 (2009).
27. Lyakin, O. Y., Bryliakov, K. P., Britovsek, G. J. P. & Talsi, E. P. EPR spectroscopic trapping of the active species of nonheme iron-catalyzed oxidation. *J. Am. Chem. Soc.* **131,** 10798–10799 (2009).
28. Ho, R. Y. N., Roelfes, G., Feringa, B. L. & Que, L. Jr Raman evidence for a weakened O–O bond in mononuclear low-spin iron(III)-hydroperoxides. *J. Am. Chem. Soc.* **121,** 264–265 (1999).
29. Bassan, A., Blomberg, M. R. A., Siegbahn, P. E. M. & Que, L. Jr A density functional study of O–O bond cleavage for a biomimetic non-heme iron complex demonstrating an Fe(V)-intermediate. *J. Am. Chem. Soc.* **124,** 11056–11063 (2002).
30. Quinonero, D., Morokuma, K., Musaev, D. G., Mas-Balleste, R. & Que, L. Jr Metal-peroxo versus metal-oxo oxidants in non-heme iron-catalyzed olefin oxidations: computational and experimental studies on the effect of water. *J. Am. Chem. Soc.* **127,** 6548–6549 (2005).
31. Ensing, B., Buda, F. & Baerends, E. J. Fenton-like chemistry in water: oxidation catalysis by Fe(III) and H_2O_2. *J. Phys. Chem. A* **107,** 5722–5731 (2003).
32. Chow, T. W-S. *et al.* *Cis*-dihydroxylation of alkenes with Oxone catalyzed by iron complexes of a macrocyclic tetraaza ligand and reaction mechanism by ESI-MS spectrometry and DFT calculations. *J. Am. Chem. Soc.* **132,** 13229–13239 (2010).
33. Comba, P., Rajaraman, G. & Rohwer, H. A. Density functional theory study of the reaction of the biomimetic iron(II) complex of a tetradentate bispidine ligand with H_2O_2. *Inorg. Chem.* **46,** 3826–3838 (2007).
34. Bukowski, M. R. *et al.* Catalytic epoxidation and 1,2-dihydroxylation of olefins with bispidine-iron(II)/H_2O_2 systems. *Angew. Chem. Int. Ed.* **45,** 3446–3449 (2006).
35. Oldenburg, P. D., Feng, Y., Pryjomska-Ray, I., Ness, D. & Que, L. Jr Olefin *cis*-dihydroxylation with bio-inspired iron catalysts. Evidence for an Fe(II)/Fe(IV) catalytic cycle. *J. Am. Chem. Soc.* **132,** 17713–17723 (2010).
36. Company, A. *et al.* Modelling the *cis*-oxo-labile binding site motif of non-heme iron oxygenases. Water exchange and remarkable oxidation reactivity of a novel non-heme iron(IV)-oxo compound bearing a tripodal tetradentate ligand. *Chem. Eur. J.* **17,** 1622–1634 (2010).

Acknowledgements

We thank the Engineering and Physical Sciences Research Council and WestCHEM for funding, and Bruker Daltonics for collaboration. L.C. thanks the Royal Society and Wolfson Research for a merit award. M.C. and X.R. thank the Ministerio de Ciencia e Innovación (MICINN) for Project CTQ2009-08464, and Generalitat de Catalunya for Institució Catalana de Recerca i Estudis Avançats Academia Awards. M.C. thanks the European Research Foundation for Project ERC-2009-StG-239910. I.P. thanks MICINN for a PhD grant. L.C. and M.C. thank COST Action D40.

Author contributions

L.C. and M.C. devised the initial concept for the work, L.C., M.C., X.R., J.S.M., I.P., J.M.L. and M.G. designed the experiments and J.S.M., M.G. and I.P. carried out the experiments and analysed the data. M.C. and L.C. co-wrote the manuscript.

Additional information

The authors declare no competing financial interests. Supplementary information and chemical compound information accompany this paper at www.nature.com/naturechemistry. Reprints and permission information is available online at http://www.nature.com/reprints. Correspondence and requests for materials should be addressed to L.C. and M.C.